



Supplement of

The effect of amino acids on the Fenton and photo-Fenton reactions in cloud water: unraveling the dual role of glutamic acid

Peng Cheng et al.

Correspondence to: Marcello Brigante (marcello.brigante@uca.fr)

The copyright of individual parts of the supplement might differ from the article licence.

Supplementary sections

Sect. S1

1.1 Kinetic data processing method of Fenton reaction

To calculate the reactivity constant of the Fenton reaction, the experimental data were analyzed using Origin 2019 software. First, the Fe(II) concentration was plotted as a function of time, and this data was fitted using a nonlinear fitting model. We selected “Exponential” as the category and used “ExpDec 1” as the fitting function. The initial reaction rate of Fe(II), represented as $(-\frac{d[Fe(II)]}{dt})$, was determined from the slope of the tangent curve at t_0 . This initial rate, obtained from the tangent's slope at t_0 , allows us to calculate the reactivity constant for the Fenton reaction as follows:

$$-\frac{d[Fe(II)]}{dt} = k_{Fe(II)/H_2O_2} \times ([Fe(II)] - [Fe(II)-Glu]) \times [H_2O_2] + k_{Fe(II)-Glu/H_2O_2} \times [Fe(II)-Glu] \times [H_2O_2] \quad (\text{eq S1})$$

$$\frac{\frac{d[Fe(II)]}{dt}}{[H_2O_2]} = k_{Fe(II)/H_2O_2} \times ([Fe(II)] - [Fe(II)-Glu]) + k_{Fe(II)-Glu/H_2O_2} \times [Fe(II)-Glu] \quad (\text{eq S2})$$

Considering that the concentration of Fe(II)-Glu is much lower than that of free Fe(II), we can simplify the reaction kinetics to primarily involve the free Fe(II) species.

$$\frac{\frac{d[Fe(II)]}{dt}}{[H_2O_2]} = k_{Fe(II)/H_2O_2} \times [Fe(II)] + k_{Fe(II)-Glu/H_2O_2} \times [Fe(II)-Glu] \quad (\text{eq S3})$$

Which, after rearrangement gives:

$$\frac{-\frac{d[Fe(II)]}{dt}}{[H_2O_2][Fe(II)]} = k_{Fe(II)/H_2O_2} + k_{Fe(II)-Glu/H_2O_2} \times \frac{[Fe(II)-Glu]}{[Fe(II)]} \quad (\text{eq S4})$$

Hence, data obtained by plotting $\frac{\frac{d[Fe(II)]}{dt}}{[H_2O_2][Fe(II)]}$ as function of $\frac{[Fe(II)-Glu]}{[Fe(II)]}$ can be fitted with a linear equation $y = ax + b$ where b is equal to $k_{Fe(II)/H_2O_2}$ and a is equal to the reactivity constant of reaction between Fe(II)-Glu complex and H_2O_2 ($k_{Fe(II)-Glu/H_2O_2}$).

1.2 ESR experiment

The mixed solution was injected into a capillary glass tube with a diameter of 0.864 mm and inserted into a highly sensitive cavity for analysis. ESR spectroscopy was performed on a Bruker EMX-plus spectrometer using the resonator 4119HS. ESR spectra were recorded at room temperature under the following operating conditions: microwave frequency 9.853 GHz, modulation amplitude 1.00 G, magnetic field scan 150 G, sweep time 15 s, conversion time 10 ms, time constant 5 ms, 2 accumulations. Spectra were acquired in the field delay mode at 1 s

scan delay. A Cr^{3+} intensity marker ($g = 1.98$, Bruker) was used in all experiments. The Xenon spin-fit embedded in the Bruker software Xenon was applied for quantification of radicals.

Sect. S2

2.1 Calculation of Fe(III) photolysis quantum yield

To obtain the Fe(II) quantum yields of the photolysis of the Fe(III) process, the generated Fe(II) concentration during the reaction was determined using the Ferrozine method. The polychromatic irradiations were carried out from 285-520 nm. The light intensity (E , $\mu\text{W cm}^{-2} \text{ s}^{-1}$) was measured using a previously calibrated spectrophotometer (Ocean Optics USB 2000+UV-Vis) coupled with an optical fiber. The photonic flux (I_0) of the polychromatic irradiation at every nm wavelength (λ) was calculated as follows

$$E = \frac{hc}{\lambda} \quad (\text{eq S5})$$

$$I_0 = \frac{E \times \lambda}{h \times c} = \frac{E \times \lambda}{1.986 \times 10^{-10}} \quad (\text{eq S6})$$

Where E represents the light intensity (E , $\mu\text{W cm}^{-2} \text{ s}^{-1}$), λ represents the wavelength (nm), h represents Planck's constant which is approximately equal to $6.62 \times 10^{-34} \text{ J s}$, $c = 3.0 \times 10^8 \text{ m s}^{-1}$ is the light speed, and I_0 is the number of the photons entering the reactor per second.

$$I_a = I_0 \times (1 - 10^{-\text{OD}_{\lambda, \text{irr}}}) \quad (\text{eq S7})$$

where $1 - 10^{-\text{OD}_{\lambda, \text{irr}}}$ represents the percentage of the light absorption by the solution at the irradiation wavelength at $t = 0\text{s}$.

Under these conditions, the effective quantum yield of Fe(II) is equal to :

$$\Phi_{\text{Fe(II)}} = \frac{d[\text{Fe(II)}] \times 6.023 \times 10^{20} \times l}{dt \times I_a} \quad (\text{eq S8})$$

Where l is the length of the irradiation cell (cm), which is equal to 6 cm in our system. $d[\text{Fe(II)}]/dt$ is the rate of Fe(II) generation during the initial irradiation period. For the quantum yield determination, the experimental error was estimated to be 5%.

2.2 Calculation of Fe(III)-Glu photolysis quantum yield

To calculate the Fe(II) quantum yield during Fe(III)-Glu photolysis, the same photolysis experiments were conducted in the presence of various concentrations of Glu. Under these conditions, the generation of Fe(II) in the system arises from the photolysis of Fe(III) and Fe(III)-Glu. Therefore, the apparent Fe(II) quantum yield for the system, $\Phi_{\text{Fe(II)}}^{\text{obs}}$, can be expressed as:

$$\Phi_{\text{Fe(II)}}^{\text{obs}} = \chi_{\text{Fe(III)}} \times \Phi_{\text{Fe(II)}}^{\text{Fe(III)}} + \chi_{\text{Fe(III)-Glu}} \times \Phi_{\text{Fe(II)}}^{\text{Fe(III)-Glu}} \quad (\text{eq S9})$$

Where $\chi_{\text{Fe(III)}}$ and $\chi_{\text{Fe(III)-Glu}}$ represent the respective fractions of Fe(III) and Fe(III)-Glu in the system, constrained by the relation:

$$\chi_{\text{Fe(III)}} + \chi_{\text{Fe(III)-Glu}} = 1 \quad (\text{eq S10})$$

By substituting $\chi_{\text{Fe(III)}} = 1 - \chi_{\text{Fe(III)-Glu}}$ into the original equation, we derive:

$$\Phi_{\text{Fe(II)}}^{\text{obs}} = \Phi_{\text{Fe(II)}}^{\text{Fe(III)}} + (\Phi_{\text{Fe(II)}}^{\text{Fe(III)-Glu}} - \Phi_{\text{Fe(II)}}^{\text{Fe(III)}}) \times \chi_{\text{Fe(III)-Glu}} \quad (\text{eq S11})$$

This equation indicates that the apparent Fe(II) quantum yield, $\Phi_{\text{Fe(II)}}^{\text{obs}}$, can be linearly related to $\chi_{\text{Fe(III)-Glu}}$. When plotting $\Phi_{\text{Fe(II)}}^{\text{obs}}$ as a function of $\chi_{\text{Fe(III)-Glu}}$, the resulting data can be fitted with a linear equation of the form: $y = ax + b$. Where b is equal to $\Phi_{\text{Fe(II)}}^{\text{Fe(III)}}$, representing the Fe(II) quantum yield during the Fe(III) photolysis. and a is equal to $(\Phi_{\text{Fe(II)}}^{\text{Fe(III)-Glu}} - \Phi_{\text{Fe(II)}}^{\text{Fe(III)}})$, which corresponds to the difference in quantum yield between Fe(III) photolysis and Fe(III)-Glu photolysis.

Sect. S3

3.1 Correction Method of Complex Stability Constant

To estimate the activity coefficient (γ_i), the Davis equation was utilized and shown as follows:

$$\text{Log } \gamma_i = -0.51 z_i^2 \left[\frac{\sqrt{I'}}{1 + \sqrt{I'}} - 0.3I' \right] \quad (\text{eq S12})$$

Where the subscript i refers to each of the reactants and products in the reactions, z_i is the ionic charge of each species, and I' is the ionic strength reported in the database. The calculated activity coefficients were then used to correct the stability constant to an ionic strength of 0 M using the following relationship:

$$K_{I=0} = K_I \frac{\prod_i \gamma_{i, \text{products}}^{\nu_i}}{\prod_i \gamma_{i, \text{reactants}}^{\nu_i}} \quad (\text{eq S13})$$

Where ν represents the stoichiometric coefficient of the reactants or products.

To correct the stability constant to a temperature of 25°C, the standard enthalpy of reaction (ΔH_r^0) and the van't Hoff equation were used:

$$\log K_{25^\circ\text{C}} = \log K_T + \Delta H_r^0 (25-T)(0.000588) \quad (\text{eq S14})$$

where T is the temperature at which $\log K$ is reported, in degrees Celsius.

Sect. S4

4.1 Determination of Fe(II)

Iron (II) concentration was determined by using Ferrozine, which forms a stable magenta complex with Fe(II) (Fe(II)-ferrozine) at a pH range from 4 to 9 (Gabet et al., 2023). The 0.1 M buffer solution of potassium phosphate was used to maintain a pH equal to 7. Different concentrations of FeSO₄ solution were used as Fe(II) sources to make the calibration curve. The molar absorption coefficient was determined to be 27850 M⁻¹ cm⁻¹, which is nearly constant to the reference value at 562 nm of 28000 M⁻¹ cm⁻¹ (Stookey, 1970).

4.2 Determination of the consumption of H₂O₂

The concentrations of hydrogen peroxide were determined by using a spectrofluorimetric quantification method (Miller and Kester, 1988). According to the literature, H₂O₂ would react with p-hydroxyphenylacetic acid (HPAA) to produce the stable p-hydroxyphenylacetic acid dimer under the catalysis of peroxidase at neutral pH which was an enzyme characterized by its selectivity toward hydroperoxides. Briefly, 0.1 mL sample was added to a mixture of 2 mL of 1 mM HPAA, 1 mL of a phosphate buffer solution (0.1 M, pH = 7.0), 3 mL pure water, and a small amount of horseradish peroxidase (POD). The sample was measured using a Varian Cary Eclipse fluorescence spectrophotometer at 408 nm for an excitation wavelength set at 320 nm.

4.3 Determination of the Acetone generation

The concentration of generated acetone in the solution was evaluated by HPLC (Shimadzu NEXERA XR HPL) equipped with a photodiode array detector and an autosampler. Samples were derivatized with DNPH and placed in the autosampler at 5 °C for 45 min before the injection (Wang et al., 2005). The column was a Macherey Nagel EC 150/4.6 NUCLEODUR 100-3 C18ec (150 mm × 4.6 mm, 3 μm particle size). The analysis of Acetone was performed using methanol (MeOH, solvent B) and water (solvent A) as mobile phase at a flow rate of 1.20 mL min⁻¹. The elution was performed using the following gradient: 70 % of B for 2 min, linear increase of B to 95 % in 5 min, then decrease of B to 70 % in 0.1 min, 70 % of B for 3 min.

To analyze acetone concentration, the samples must be derivatized with DNPH. To obtain the DNPH solution, 2.5 mL pure hydrochloric acid, 1.25 mL acetonitrile, and 6.25 mL H₂O were added sequentially into a 10 mL centrifuge tube containing 0.04 g of the DNPH solid. 20 μL DNPH solution should be mixed with 1 mL samples for derivatization. Then the mixed solution must be placed in the autosampler at 5 °C for 45 min before the injection.

Sect. S5

5.1 Analysis of HPLC-MS

The quantification of Glutamic acid (Glu) and the identification of its transformation products were conducted using a ThermoScientific Orbitrap Q-Exactive high-resolution mass spectrometry (HRMS) coupled with a ThermoScientific Ultimate 3000 RSLC ultra-high-performance liquid chromatography (UPLC) system. Analyses were performed in both negative and positive electrospray modes (ESI^+ and ESI^-). The chromatographic separation was achieved using a Waters ACQUITY UPLC BEH Amide column (100×2.1 mm, particle size of $1.7 \mu\text{m}$) with an injection volume of $5 \mu\text{L}$. Glu and its transformation products were separated using an elution gradient method with 0.1 % formic acid water solution as solvent A and acetonitrile (ACN) with 0.1 % formic acid as solvent B as mobile phase at a flow rate of 0.40 mL min^{-1} . The elution followed a specific gradient profile: the initial condition set B at 90% at 0 min, with a linear decrease to 58 % in 8 min, further reduction to 50 % in 0.1 min, and maintained at 50 % B for 0.9 min. Subsequently, B was increased to 90 % in 0.1 min and maintained at 90 % B for 2.9 min.

5.2 Analysis of IC-MS

The quantification of carboxyl acid and ammonium (NH_4^+) was determined using ion chromatography using a Thermo-Fisher Scientific ICS-6000 Ionic chromatograph equipped with with a simple quadrupole mass spectrometer (ISQ-EC-Thermo Scientific). The Dionex IonPac AS-11-HC- $4 \mu\text{m}$ 2×250 mm column was employed and the KOH gradient initiated at 1 mM KOH from 0 to 5 min, increased to 30 mM KOH from 5.1 to 25 min, and further elevated to 60 mM KOH from 25.1 to 31 min. This concentration was held until 35 min, after which the column was re-equilibrated at 1 mM KOH at 35.1 min. The flow rate of 0.36 mL min^{-1} and temperature of 40°C were set. The simple quadrupole mass spectrometer operated in negative ion mode using electrospray ionization with an ESI capillary voltage of 3000 V. Full scan analysis (10-500 m/z) and targeted analysis ($\pm 0.5 \text{ amu}$) were conducted to facilitate the characterization and quantification of each product. IonPac CG-16 (guard column 2×50 mm) and an Ion-Pac CS16 (analytical column 2×250 mm) for cations. Isocratic elution with MSA (methanesulfonic acid at 30 mM) at a flow rate of 0.25 mL min^{-1} was employed. Chromatograms were recorded with a conductometric cell detector and analyzed with Chromeleon 7.2 software (Thermo Scientific). The concentrations were measured in triplicate. All carboxylic acids concentrations are provided as “total” concentration considering that for all compounds different protonated/deprotonated forms exist in solution as function of pK_a and pH.

5.3 Analysis of TOC

The total organic carbon (TOC) concentration in the aqueous solution was followed by a Shimadzu TOC 5050A analyzer. For each experimental sample (8 mL), two injections are conducted, and the average of these two measurements is initially recorded as the TOC concentration. If the deviation between the first two injection results exceeds 5 %, a third injection is performed. In such cases, the TOC concentration is calculated as the average of all valid injection results. In this study, TOC was determined by calculating the difference between the measured total carbon (TC) and inorganic carbon (IC) concentrations:

$$\text{TOC} = \text{TC} - \text{IC} \quad (\text{eq S15})$$

Figures



Fig. S1 Home-made Pyrex jacketed cylindrical photo-reactor.

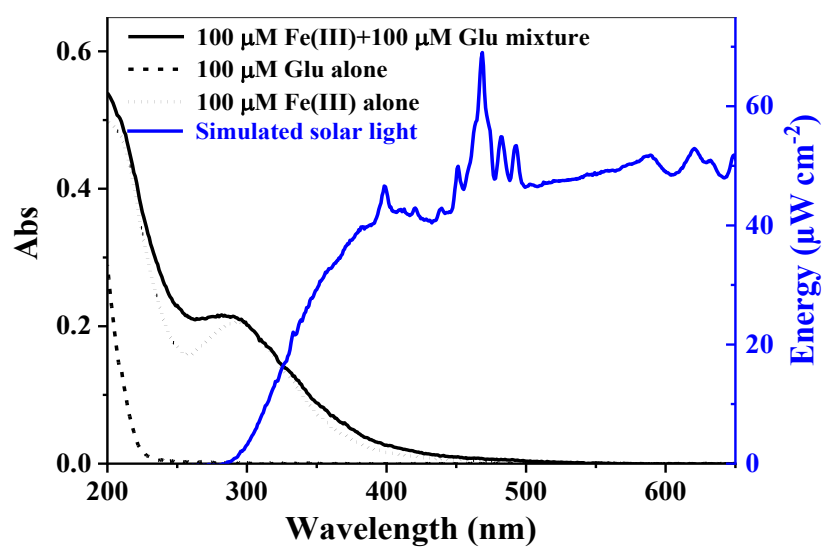


Fig. S2 UV-Visible spectra of Fe(III), Glu, and Fe(III)-Glu mixture (black curves) at pH = 3.7, and emission spectrum of simulated solar light (blue curve).

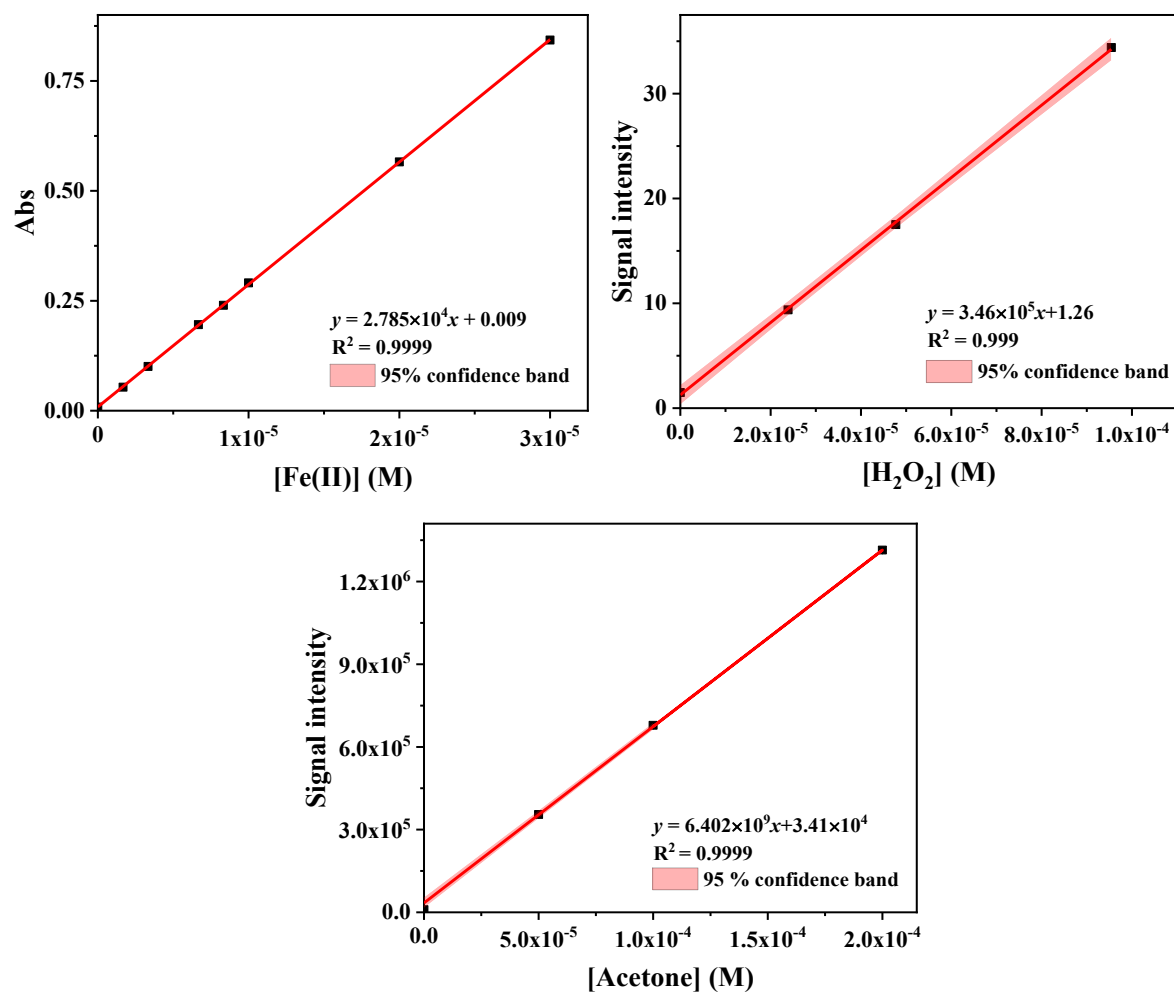


Fig. S3 a) Calibration curve of Fe(II) using the complexation with Ferrozine and detection of the complex at 562 nm; b) The calibration curve of H_2O_2 concentration; c) The calibration curve of Acetone.

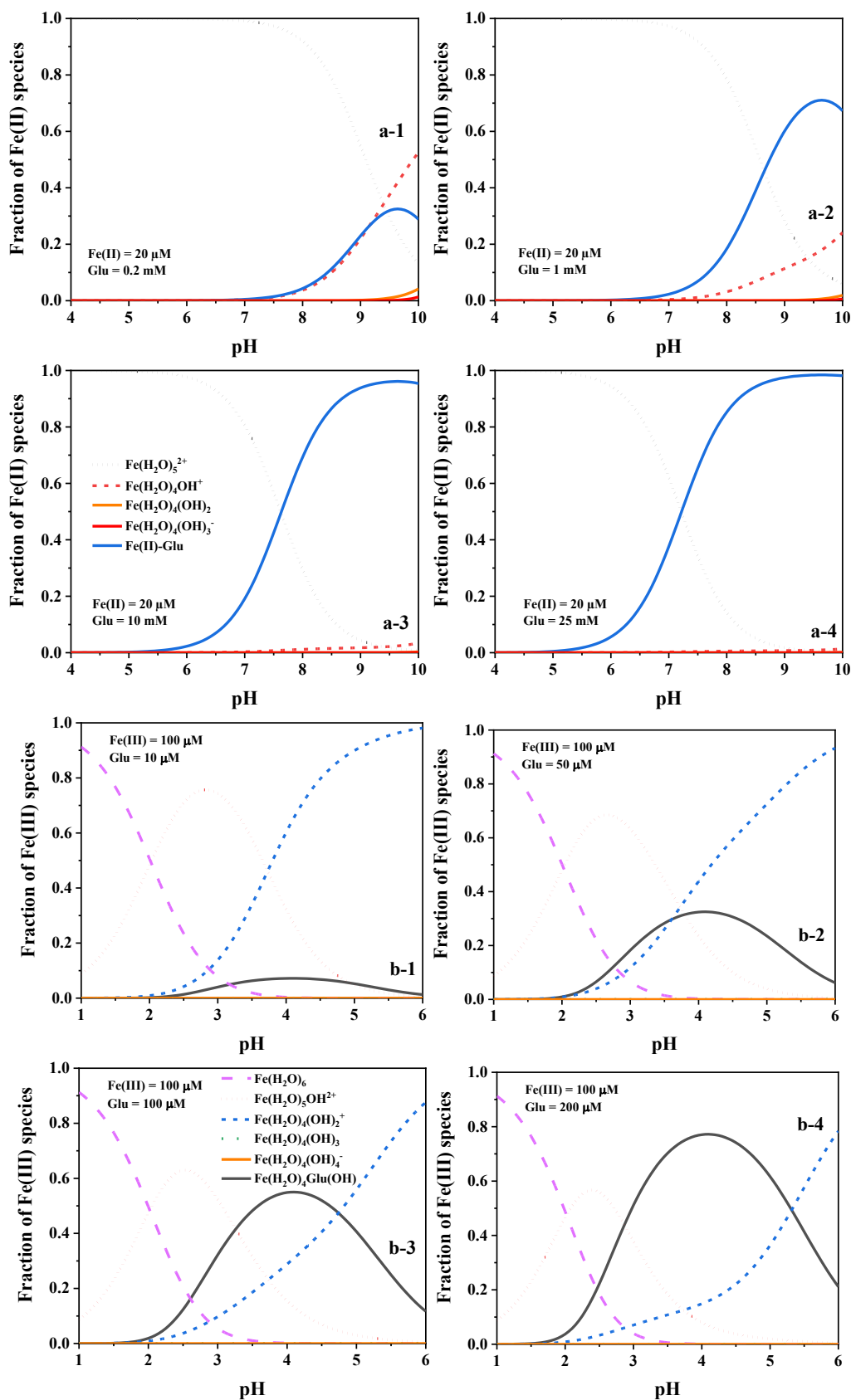


Fig. S4 Speciation of Fe(II) and Fe(III) in the presence of varying Glu concentrations at different pH
a1-4) $[\text{Fe(II)}] = 20 \mu\text{M}$, $[\text{Glu}] = 0.2\text{-}25 \text{ mM}$; **b1-4)** $[\text{Fe(III)}] = 100 \mu\text{M}$, $[\text{Glu}] = 20\text{-}100 \mu\text{M}$.

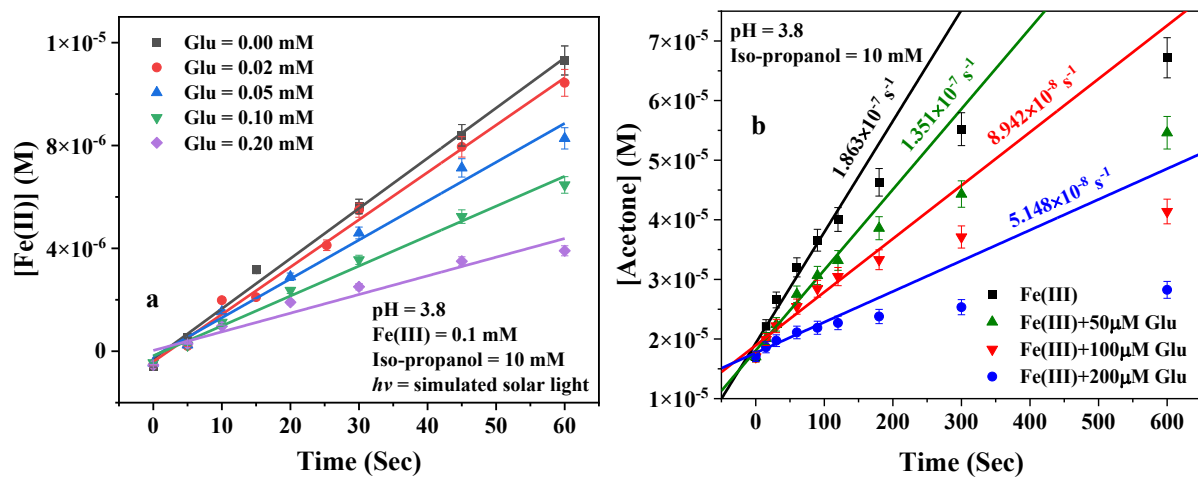


Fig. S5 a) Fe(II) generation rate of Fe(III) photolysis in the presence of different Glu concentrations. **b)** Acetone generation rate of Fe(III) photolysis in the presence of different Glu concentrations and isopropanol.

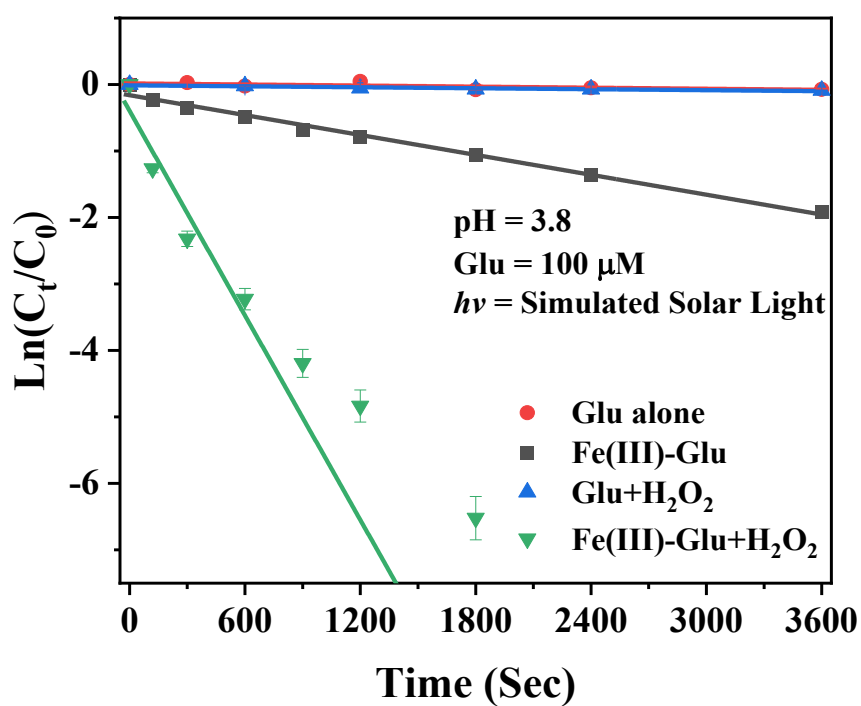


Fig. S6 Degradation of glutamic acid (GLU) by simulated solar light in the aqueous phase.

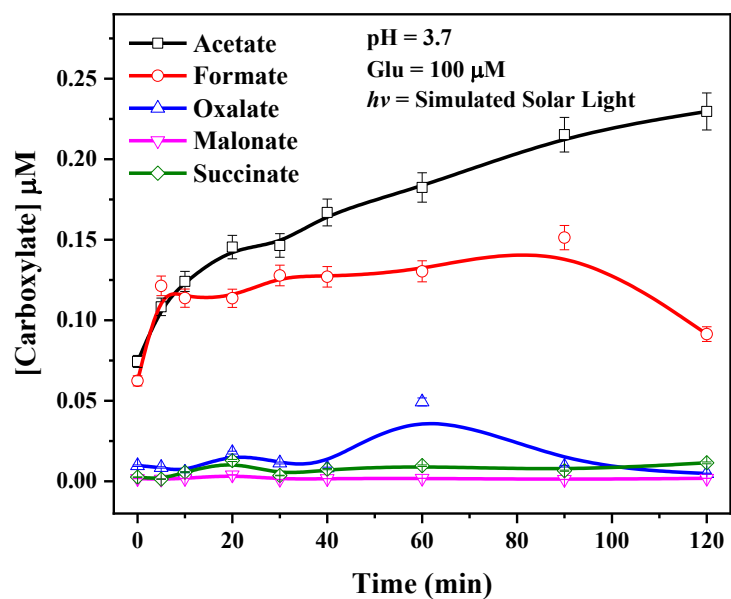


Fig. S7 Formation of carboxylic acids through the photolysis of Glu by simulated solar light.

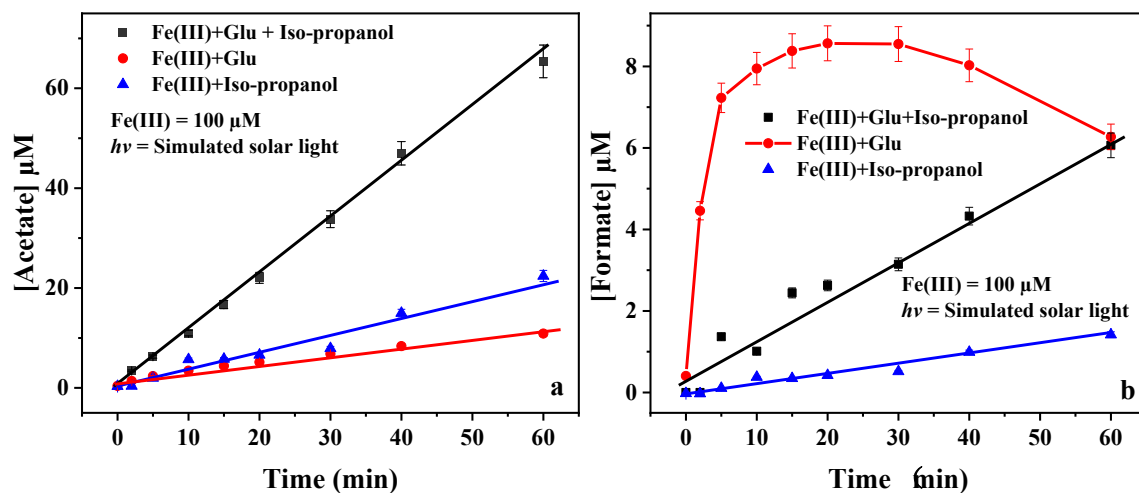


Fig. S8 Comparison of **a)** acetate and **b)** formate formation in the Fe(III)-Glu system in the absence and presence of isopropanol. (black curve: [Fe(III)] = 100μM, [Glu] = 100 μM, [Iso-propanol] = 2.0 mM; red curve: [Fe(III)] = 100μM, [Glu] = 100 μM; blue curve: [Fe(III)] = 100μM, [Iso-propanol] = 2.0 mM)

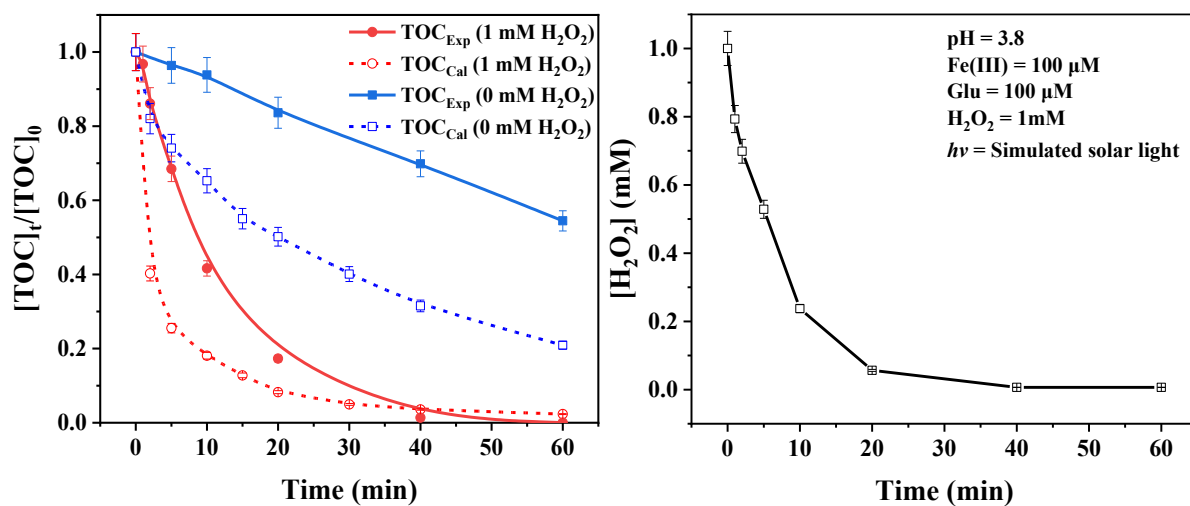


Fig. S9 a) Evolution of the TOC of the solution. **b)** H_2O_2 consumption as a function of irradiation time. $[\text{H}_2\text{O}_2] = 1 \text{ mM}$; $[\text{Glu}] = 100 \mu\text{M}$; $[\text{Fe(III)}] = 100 \mu\text{M}$

Tables

Table S1 The energy and photonic flux of the polychromatic irradiation at every nanometer from 285-520 nm.

λ_{irr} (nm)	Energy ($\mu\text{W cm}^{-2}$)	I_0 (10^{12} photons $\text{s}^{-1} \text{cm}^{-2}$)
520	47.46	124.26
519	47.21	123.37
518	47.21	123.12
517	47.18	122.81
516	47.18	122.58
515	47.08	122.10
514	47.18	122.12
513	47.14	121.77
512	46.83	120.73
511	46.68	120.11
510	46.74	120.01
509	46.59	119.41
508	46.51	118.96
507	46.58	118.92
506	46.66	118.89
505	46.76	118.91
504	46.80	118.76
503	46.92	118.82
502	46.76	118.20
501	46.53	117.38
500	46.52	117.13
499	46.40	116.57
498	46.79	117.33
497	47.10	117.86
496	47.95	119.75
495	49.90	124.38
494	52.37	130.27
493	53.40	132.57
492	53.33	132.13
491	51.84	128.17
490	49.30	121.64
489	47.97	118.11
488	47.75	117.34
487	48.62	119.21
486	49.65	121.49
485	50.95	124.43
484	53.08	129.37
483	54.82	133.32
482	54.89	133.22
481	53.95	130.67
480	51.66	124.85

479	49.19	118.64
478	47.88	115.24
477	48.08	115.48
476	50.72	121.57
475	53.79	128.65
474	55.95	133.53
473	57.09	135.97
472	58.51	139.07
471	59.75	141.71
470	62.45	147.78
469	67.93	160.41
468	68.02	160.28
467	65.54	154.12
466	60.77	142.59
465	57.61	134.89
464	57.34	133.97
463	56.67	132.11
462	54.51	126.80
461	51.62	119.83
460	50.58	117.16
459	49.98	115.52
458	48.88	112.73
457	47.43	109.15
456	46.58	106.96
455	46.11	105.64
454	46.78	106.94
453	47.46	108.25
452	48.86	111.19
451	49.71	112.90
450	47.38	107.36
449	46.04	104.10
448	44.31	99.95
447	42.71	96.14
446	42.16	94.67
445	42.30	94.79
444	42.14	94.22
443	42.17	94.06
442	41.98	93.42
441	42.25	93.81
440	42.70	94.61
439	42.71	94.41
438	42.57	93.89
437	42.07	92.58
436	41.13	90.30
435	40.76	89.28
434	40.82	89.20
433	40.72	88.78

432	40.58	88.27
431	40.85	88.66
430	40.73	88.19
429	40.93	88.41
428	41.00	88.36
427	40.85	87.83
426	41.12	88.20
425	41.13	88.02
424	41.48	88.55
423	41.70	88.83
422	42.21	89.68
421	42.80	90.74
420	42.78	90.47
419	42.30	89.23
418	41.91	88.22
417	41.72	87.59
416	41.81	87.59
415	41.86	87.48
414	42.06	87.67
413	42.47	88.33
412	42.43	88.01
411	42.30	87.54
410	42.63	88.02
409	42.56	87.64
408	42.31	86.93
407	42.17	86.42
406	42.29	86.45
405	42.30	86.27
404	42.48	86.42
403	43.09	87.45
402	43.40	87.86
401	44.83	90.52
400	45.71	92.06
399	46.52	93.46
398	46.12	92.44
397	44.99	89.93
396	43.78	87.29
395	43.29	86.10
394	42.27	83.86
393	41.25	81.63
392	40.89	80.70
391	40.37	79.48
390	40.25	79.03
389	39.94	78.23
388	40.09	78.33
387	39.87	77.69
386	39.65	77.06

385	39.73	77.02
384	39.39	76.16
383	39.71	76.58
382	39.71	76.39
381	39.12	75.04
380	39.31	75.21
379	38.72	73.88
378	38.42	73.13
377	38.01	72.16
376	37.85	71.67
375	37.52	70.84
374	37.49	70.61
373	36.90	69.31
372	36.98	69.27
371	36.54	68.26
370	35.99	67.05
369	35.80	66.51
368	35.16	65.16
367	34.70	64.11
366	34.52	63.61
365	34.11	62.69
364	34.06	62.42
363	33.65	61.50
362	33.32	60.73
361	33.02	60.02
360	32.76	59.39
359	32.72	59.15
358	32.39	58.38
357	32.08	57.67
356	31.89	57.17
355	31.22	55.80
354	30.93	55.14
353	30.71	54.58
352	30.30	53.70
351	29.61	52.34
350	29.19	51.44
349	29.07	51.09
348	28.34	49.65
347	27.75	48.49
346	27.77	48.38
345	27.40	47.60
344	26.34	45.63
343	26.20	45.25
342	25.47	43.86
341	25.21	43.29
340	24.27	41.54
339	24.16	41.24

338	23.89	40.66
337	23.35	39.63
336	22.17	37.51
335	21.62	36.47
334	21.63	36.37
333	22.10	37.06
332	20.82	34.81
331	19.10	31.83
330	18.37	30.52
329	18.00	29.83
328	17.14	28.30
327	16.80	27.66
326	16.54	27.16
325	16.07	26.31
324	15.36	25.07
323	14.42	23.45
322	13.88	22.50
321	13.82	22.34
320	13.41	21.60
319	12.67	20.35
318	12.26	19.64
317	11.73	18.72
316	10.91	17.36
315	10.23	16.23
314	9.84	15.55
313	9.76	15.38
312	8.85	13.90
311	8.26	12.94
310	7.79	12.16
309	7.33	11.40
308	6.77	10.50
307	6.00	9.27
306	5.68	8.75
305	5.30	8.14
304	4.82	7.37
303	4.30	6.56
302	3.90	5.94
301	3.68	5.58
300	3.16	4.78
299	2.79	4.20
298	2.38	3.57
297	2.27	3.40
296	2.07	3.09
295	1.74	2.59
294	1.47	2.17
293	1.15	1.70
292	0.96	1.41

291	0.86	1.26
290	0.65	0.95
289	0.51	0.74
288	0.34	0.49
287	0.23	0.34
286	0.29	0.42
285	0.02	0.03

Table S2 The detailed parameter used to obtain the speciation of Fe(III)-Glu/Fe(III)-aqua complexes using HySS2009 software.

Formula	Log β				References
Glu ²⁻	GluH ⁻	GluH ₂	GluH ₃		
	9.96	14.26	16.42		(J. P., 2013)
Fe(III)	FeOH ²⁺	Fe(OH) ₂ ⁺	Fe(OH) ₃	Fe(OH) ₄ ⁻	
	-2.02	-5.75	-15	-22.7	(J. P., 2013)
Fe(III)-Glu	Fe(III)-Glu ⁺				
	13.39				(J. P., 2013)
Fe(II)	FeOH ⁺	Fe(OH) ₂ ⁺	Fe(OH) ₃ ⁻		
	-9.397	-20.494	-30.991		(J. P., 2013)
Fe(II)-Glu	Fe(II)-Glu				
	4.336				(J. P., 2013; Perrin, 1959)
H ₂ O	OH ⁻				
	13.999				(Pastina and LaVerne, 2001)

Ionic strength = 0 M, Temperature = 25 °C

Table S3 Chemical reactions and reactivity constants used in the COPASI software.

Equations	Comments	k (M ⁻¹ s ⁻¹ or s ⁻¹)	References
HO_x Equilibrium	K		
H ₂ O = H ⁺ + OH ⁻	$pK_a = 13.999$	→2.53E-05	Calculated
	$K = 1.002E-14$	←1.40E+11	(Pastina and LaVerne, 2001)
H ₂ O ₂ = HO ₂ ⁻ + H ⁺	$pK_a = 11.65$	→1.12E-01	Calculated

	2.239E-12	←5.00E+10	(Pastina and LaVerne, 2001)
$\bullet\text{OH} = \text{H}^+ + \text{O}^-$	$pK_a = 11.9$	→1.26E-01	Calculated
	1.259E-12	←1.00E+11	(Pastina and LaVerne, 2001)
$\text{HO}_2\bullet = \text{H}^+ + \text{O}_2^-$	$pK_a = 4.57$	→1.35E+06	Calculated
	2.692E-05	←5.00E+10	(Pastina and LaVerne, 2001)
Fe(II) Equilibrium			
$\text{Fe(II)} + \text{H}_2\text{O} = \text{Fe(OH)}^+ + \text{H}^+$	4.009E-10	4.70E+04	(Herrmann et al., 1999)
	←	1.17E+14	Calculated
$\text{Fe(OH)}^+ + \text{H}_2\text{O} = \text{Fe(OH)}_2 + \text{H}^+$	7.998E-12	1.10E+03	(Herrmann et al., 1999)
	←	1.38E+14	Calculated
$\text{Fe(OH)}_2 + \text{H}_2\text{O} = \text{Fe(OH)}_3^- + \text{H}^+$	3.184E-11	1.10E+03	(Herrmann et al., 1999)
		3.46E+13	calculated
Fe(III) Equilibrium			
$\text{Fe(III)} + \text{H}_2\text{O} = \text{Fe(OH)}^{2+} + \text{H}^+$	6.501E-03	4.70E+04	(Herrmann et al., 1999)
	←	7.23E+06	Calculated
$\text{Fe(OH)}^{2+} + \text{H}_2\text{O} = \text{Fe(OH)}_2^+ + \text{H}^+$	3.917E-03	1.10E+03	(Herrmann et al., 1999)
	←	2.81E+05	Calculated
$\text{Fe(OH)}_2^+ + \text{H}_2\text{O} = \text{Fe(OH)}_3 + \text{H}^+$	1.081E-08	1.10E+03	(Herrmann et al., 1999)
	←	1.02E+11	Calculated
$\text{Fe(OH)}_3 + \text{H}_2\text{O} = \text{Fe(OH)}_4^- + \text{H}^+$	9.376E-10	1.10E+03	(Herrmann et al., 1999)
	←	1.17E+12	Calculated
Glu Dissociation Equilibrium			
$\text{H}_3\text{Glu}^+ = \text{H}^+ + \text{H}_2\text{Glu}$	5.888E-03	2.94E+08	Calculated
	←	5.00E+10	Estimated from Capram2.3 (Herrmann et al., 1999)
$\text{H}_2\text{Glu} = \text{H}^+ + \text{HGlu}^-$	3.802E-05	1.90E+06	Calculated
	←	5.00E+10	Estimated from Capram2.3 (Herrmann et al., 1999)
$\text{HGlu}^- = \text{H}^+ + \text{Glu}^{2-}$	1.122E-10	5.61E+00	Calculated
	←	5.00E+10	Estimated from

			Capram2.3 (Herrmann et al., 1999)
Fe(II)-Glu complexation Equilibrium			
$\text{Fe(II)} + \text{Glu}^{2-} = \text{FeGlu}$	2.168E+04	7.50E+06	Estimated from Capram2.3 (Herrmann et al., 1999)
		3.46E+02	Calculated
Acid-base Reactions			
$\text{H}_2\text{O}_2 + \text{OH}^- = \text{HO}_2^- + \text{H}_2\text{O}$		1.30E+10	(Pastina and LaVerne, 2001)
	←	3.23E+09	
$\text{HO}_2^\bullet + \text{OH}^- = \text{H}_2\text{O} + \text{O}_2^-$	→	5.00E+10	(Pastina and LaVerne, 2001)
	←	1.76E+03	
$^\bullet\text{OH} + \text{OH}^- = \text{H}_2\text{O} + \text{O}^-$	→	1.30E+10	(Pastina and LaVerne, 2001)
	←	5.75E+09	
$\text{Fe(II)} + \text{H}_2\text{O}_2 \rightarrow \text{Fe(III)} + \text{OH}^- + ^\bullet\text{OH}$	Fenton reaction	6.30E+01	(Kang et al., 2002)
$\text{Fe(II)} + ^\bullet\text{OH} \rightarrow \text{Fe(III)} + \text{OH}^-$		3.20E+08	
$\text{Fe(II)} + \text{HO}_2^\bullet \rightarrow \text{Fe(III)} + \text{HO}_2^-$		1.20E+06	(Kang et al., 2002)
$\text{Fe(II)} + \text{O}_2^\bullet + \text{H}^+ \rightarrow \text{Fe(III)} + \text{HO}_2^-$		1.00E+07	(Kang et al., 2002)

Reactions with Fe(III)			
$\text{Fe(III)} + \text{H}_2\text{O}_2 \rightarrow \text{Fe(II)} + \text{HO}_2^\bullet + \text{H}^+$	Fenton-like reaction	1.00E-02	(Kang et al., 2002)
$\text{Fe(III)} + \text{HO}_2^\bullet \rightarrow \text{Fe(II)} + \text{O}_2 + \text{H}^+$		3.30E+05	
$\text{Fe(III)} + \text{O}_2^\bullet \rightarrow \text{Fe(II)} + \text{O}_2$		5.00E+07	(Kang et al., 2002)
Reactions with HO_x			
$^\bullet\text{OH} + \text{H}_2\text{O}_2 \rightarrow \text{H}_2\text{O} + \text{HO}_2^\bullet$		2.70E+07	(Pastina and LaVerne, 2001)
$^\bullet\text{OH} + \text{HO}_2^\bullet \rightarrow \text{O}_2 + \text{H}_2\text{O}$		1.00E+10	(Kang et al., 2002)
$2 ^\bullet\text{OH} \rightarrow \text{H}_2\text{O}_2$	2 <i>k</i>	4.20E+09	(Kang et al., 2002)
$^\bullet\text{OH} + \text{HO}_2^- \rightarrow \text{HO}_2^\bullet + \text{OH}^-$		7.50E+09	(Pastina and LaVerne, 2001)
$^\bullet\text{OH} + \text{O}_2^\bullet \rightarrow \text{O}_2 + \text{OH}^-$		1.00E+10	(Kang et al., 2002)

$\text{HO}_2^\bullet + \text{H}_2\text{O}_2 \rightarrow \text{H}_2\text{O} + \text{O}_2 + \bullet\text{OH}$		5.00E-01	(Pastina and LaVerne, 2001)
$2 \text{HO}_2^\bullet \rightarrow \text{H}_2\text{O}_2 + \text{O}_2$	2k	8.30E+05	(Kang et al., 2002)
$\text{HO}_2^\bullet + \text{O}_2^\bullet \rightarrow \text{HO}_2^- + \text{O}_2$		9.70E+07	(Kang et al., 2002)
$\text{O}_2^\bullet + \text{H}_2\text{O}_2 \rightarrow \bullet\text{OH} + \text{OH}^- + \text{O}_2$		1.60E+01	(Ivanova et al., 2012)
$2 \text{O}_2^\bullet + 2 \text{H}_2\text{O} \rightarrow \text{H}_2\text{O}_2 + \text{O}_2 + 2\text{OH}^-$	2k	3.20E-02	(Pastina and LaVerne, 2001)
Reaction with Phenol and its products			
$\text{C}_6\text{H}_5\text{OH} \rightarrow \text{C}_6\text{H}_5\text{O}^\bullet + \text{H}^+$		5.00E+00	(Hoffmann et al., 2018)
$\text{C}_6\text{H}_5\text{O}^\bullet + \text{H}^+ \rightarrow \text{C}_6\text{H}_5\text{OH}$		5.00E+10	(Hoffmann et al., 2018)
$\bullet\text{OH} + \text{C}_6\text{H}_5\text{OH} \rightarrow 0.92 \text{ PHENHCHD}^\bullet + 0.08 \text{ C}_6\text{H}_5\text{O}^\bullet$		3.30E+09	(Hoffmann et al., 2018)
$\text{PHENHCHD}^\bullet + \text{H}^+ \rightarrow \text{C}_6\text{H}_5\text{OH}^+ + \text{H}_2\text{O}$	Reversible	5.00E+08	(Hoffmann et al., 2018)
$\text{C}_6\text{H}_5\text{OH}^+ + \text{H}_2\text{O} \rightarrow \text{PHENHCHD} + \text{H}^+$		2.00E+07	(Hoffmann et al., 2018)
$\text{PHENHCHD}^\bullet + \text{O}_2 \rightarrow 0.5 \text{ 1,2-C}_6\text{H}_4(\text{OH})_2 + 0.5 \text{ 1,4-C}_6\text{H}_4(\text{OH})_2 + \text{HO}_2^\bullet$		1.20E+09	(Hoffmann et al., 2018)
$\text{Fe(III)} + \text{PHENHCHD}^\bullet \rightarrow 0.5 \text{ 1,2-C}_6\text{H}_4(\text{OH})_2 + 0.5 \text{ 1,4-C}_6\text{H}_4(\text{OH})_2 + \text{H}^+ + \text{Fe(II)}$		7.00E+03	(Hoffmann et al., 2018)
$2 \text{ PHENHCHD} \rightarrow 0.5 \text{ 1,2-C}_6\text{H}_4(\text{OH})_2 + 0.5 \text{ 1,4-C}_6\text{H}_4(\text{OH})_2 + \text{C}_6\text{H}_5\text{OH}$	2k	1.00E+08	(Hoffmann et al., 2018)
$2 \text{ PHENHCHD} + \bullet\text{OH} \rightarrow \text{THB}$	THB = tri-hydroxy benzene	2.00E+10	(Pontes et al., 2010)
$\text{C}_6\text{H}_5\text{OH}^+ \rightarrow \text{C}_6\text{H}_5\text{O}^\bullet + \text{H}^+$		5.00E+12	(Hoffmann et al., 2018)
$\text{C}_6\text{H}_5\text{O}^\bullet + \text{H}^+ \rightarrow \text{C}_6\text{H}_5\text{OH}^+$		5.00E+10	(Hoffmann et al., 2018)
$\text{C}_6\text{H}_5\text{OH}^+ + \text{H}_2\text{O} \rightarrow \text{PHENHCHD}^\bullet + \text{H}^+$	Reversible	2.00E+07	(Hoffmann et al., 2018)
$\text{PHENHCHD}^\bullet + \text{H}^+ \rightarrow \text{C}_6\text{H}_5\text{OH}^+ + \text{H}_2\text{O}$		5.00E+08	(Hoffmann et al., 2018)
$\text{C}_6\text{H}_5\text{OH}^+ + \text{Fe(II)} \rightarrow \text{C}_6\text{H}_5\text{OH} + \text{Fe(III)}$		6.00E+08	(Hoffmann et al., 2018)
$\text{C}_6\text{H}_5\text{O}^\bullet + \text{HO}_2^\bullet \rightarrow \text{C}_6\text{H}_5\text{OH} + \text{O}_2$		2.00E+09	(Hoffmann et al., 2018)
$\text{C}_6\text{H}_5\text{O}^\bullet + \text{O}_2^\bullet + \text{H}^+ \rightarrow \text{1,4-C}_6\text{H}_4\text{O}_2 + \text{H}_2\text{O}$		1.00E+09	(Hoffmann et al., 2018)
$2 \text{ C}_6\text{H}_5\text{O}^\bullet \rightarrow \text{C}_{12}\text{H}_{10}\text{O}_2$	2k	2.45E+09	(Hoffmann et al., 2018)
$\text{C}_6\text{H}_5\text{O}^\bullet + \text{H}^+ \rightarrow \text{C}_6\text{H}_5\text{OH}^+$		5.00E+10	(Hoffmann et al., 2018)
$2 \text{ C}_6\text{H}_5\text{O}^\bullet + 4\text{-HOC}_6\text{H}_4\text{O}^- \rightarrow \text{C}_6\text{H}_5\text{O}^- + 4\text{-OC}_6\text{H}_4\text{O}^\bullet$		2.20E+09	(Neta and Grodkowski, 2005)

$C_6H_5O^\bullet + Fe(II) + H^+ \rightarrow C_6H_5OH + Fe(III)$		1.00E+08	(Neta and Grodkowski, 2005)
$1,2-C_6H_4(OH)_2 + \bullet OH + O_2 \rightarrow 1,2-C_6H_4O_2 + HO_2^\bullet + H_2O$		4.70E+09	(Hoffmann et al., 2018)
$1,2-C_6H_4(OH)_2 + HO_2^\bullet \rightarrow 2-HOC_6H_4O^\bullet + H_2O_2$		4.70E+04	(Hoffmann et al., 2018)
$1,2-C_6H_4(OH)_2 + O_2^\bullet + H^+ \rightarrow 2-HOC_6H_4O^\bullet + H_2O_2$		2.70E+05	(Hoffmann et al., 2018)
$1,4-C_6H_4(OH)_2 + \bullet OH + O_2 \rightarrow 1,4-C_6H_4O_2 + HO_2^\bullet + H_2O$		1.60E+10	(Hoffmann et al., 2018)
$1,4-C_6H_4(OH)_2 + HO_2^\bullet \rightarrow 4-HOC_6H_4O^\bullet + H_2O_2$		8.50E+03	(Hoffmann et al., 2018)
$1,4-C_6H_4(OH)_2 + O_2^\bullet + H^+ \rightarrow 4-HOC_6H_4O^\bullet + H_2O_2$		1.70E+07	(Hoffmann et al., 2018)
$2\ 2-HOC_6H_4O^\bullet \rightarrow 1,2-C_6H_4(OH)_2 + 1,2-C_6H_4O_2$	2k	1.09E+09	(Hoffmann et al., 2018)
$2-HOC_6H_4O^\bullet + O_2 \rightarrow 1,2-C_6H_4O_2 + HO_2^\bullet$		1.60E-02	(Hoffmann et al., 2018)
$Fe(III) + 2-HOC_6H_4O^\bullet \rightarrow 1,2-C_6H_4O_2 + H^+ + Fe(II)$		7.00E+05	(Hoffmann et al., 2018)
$Fe(III) + 2-HOC_6H_4O^\bullet + H^+ \rightarrow 1,2-C_6H_4O_2 + Fe(II)$		1.50E+05	(Hoffmann et al., 2018)
$2\ 4-HOC_6H_4O^\bullet \rightarrow 1,4-C_6H_4(OH)_2 + 1,4-C_6H_4O_2$	2k	1.09E+09	(Hoffmann et al., 2018)
$4-HOC_6H_4O^\bullet + O_2 \rightarrow 1,4-C_6H_4O_2 + HO_2^\bullet$		1.60E-02	(Hoffmann et al., 2018)
$Fe(III) + 4-HOC_6H_4O^\bullet \rightarrow 1,4-C_6H_4O_2 + H^+ + Fe(II)$		7.00E+05	(Hoffmann et al., 2018)
$Fe(III) + 4-HOC_6H_4O^\bullet + H^+ \rightarrow 1,4-C_6H_4O_2 + Fe(II)$		1.50E+05	(Hoffmann et al., 2018)

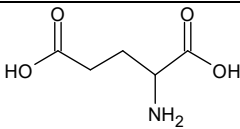
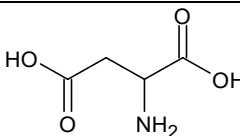
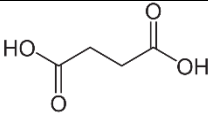
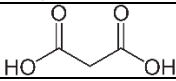
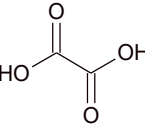
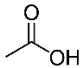
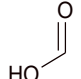
Table S4 Fraction of Fe(II)-Glu complex in the presence of different Glu concentrations at pH 5.6.

[Glu] (M)	[Fe(II)- Glu] (M)	[Fe(II) _{total}] (M)	[H ₂ O ₂] (M)	$\frac{[Fe(II)-Glu]}{[Fe(II)]}$ (%)	$-\frac{d[Fe(II)]}{dt}$	$-\frac{d[Fe(II)]}{dt}$ [H ₂ O ₂][Fe(II)]
2.00×10 ⁻⁴	3.63×10 ⁻⁹	2.0×10 ⁻⁵	1.0×10 ⁻⁴	0.02	6.28×10 ⁻⁷	340.53
1.00×10 ⁻³	1.81×10 ⁻⁸			0.09	8.34×10 ⁻⁷	378.72
6.00×10 ⁻³	1.08×10 ⁻⁸			0.54	9.73×10 ⁻⁷	479.56
1.00×10 ⁻²	1.80×10 ⁻⁷			0.90	9.65×10 ⁻⁷	481.45
1.25×10 ⁻²	2.25×10 ⁻⁷			1.12	1.19×10 ⁻⁶	577.71
1.70×10 ⁻²	3.04×10 ⁻⁷			1.52	1.12×10 ⁻⁶	556.67
2.50×10 ⁻²	4.44×10 ⁻⁷			2.22	1.44×10 ⁻⁶	695.84

Table S5 Fraction of Fe(III)-Glu complex in the presence of different Glu concentrations at pH 3.7.

[Glu] (M)	[Fe(III)-Glu] (M)	[Fe(III) _{total}] (M)	Fe(III)-Glu (%)	Fe(III) (%)	FeOH ²⁺ (%)	Fe(OH) ₂ ⁺ (%)
0.0	0	1.0×10 ⁻⁴	0.00	1.07	51.17	47.76
0.1×10 ⁻⁴	6.99×10 ⁻⁶		6.82	0.99	47.69	44.50
0.2×10 ⁻⁴	1.33×10 ⁻⁵		13.31	0.93	44.36	41.40
0.5×10 ⁻⁴	3.07×10 ⁻⁵		30.71	0.74	35.46	33.09
1.0×10 ⁻⁴	5.23×10 ⁻⁵		52.29	0.50	24.42	22.79
2.0×10 ⁻⁴	7.43×10 ⁻⁵		74.28	0.28	13.16	12.28

Table S6 UPLC-MS-MS and IC-MS data of Glu degradation products.

Compound	Rt (min)	Exp [M+H] ⁺	Theor [M+H] ⁺	Δm mu	Exp [M-H] ⁻	Theor [M-H] ⁻	Δm mu	Molecular formula	Proposed Structure
Glutamic acid (Glu)	4.52	148.0602	148.0604	0.23	146.0441	146.0448	0.64	C ₅ H ₉ O ₄ N	
Aspartic acid (Asp)	4.85	132.0288	132.0291	0.35	132.0288	132.0291	0.35	C ₄ H ₇ O ₄ N	
IC-MS									
Compound	Rt	ESI-(m/z)							
Succinic acid	27.6	117							
Malonic acid	28.2	103							
Oxalic acid	29.8	89							
Acetic acid	11.4	59							
Formic acid	12.6	45							

References

- Gabet, A., Guy, C., Fazli, A., Métivier, H., de Brauer, C., Brigante, M., and Mailhot, G.: The ability of recycled magnetite nanoparticles to degrade carbamazepine in water through photo-Fenton oxidation at neutral pH, *Separation and Purification Technology*, 317, 123877, <https://doi.org/10.1016/j.seppur.2023.123877>, 2023.
- Herrmann, H., Ervens, B., Nowacki, P., Wolke, R., and Zellner, R.: A chemical aqueous phase radical mechanism for tropospheric chemistry, *Chemosphere*, 38, 1223–1232, [https://doi.org/10.1016/S0045-6535\(98\)00520-7](https://doi.org/10.1016/S0045-6535(98)00520-7), 1999.
- Hoffmann, E. H., Tilgner, A., Wolke, R., Böge, O., Walter, A., and Herrmann, H.: Oxidation of substituted aromatic hydrocarbons in the tropospheric aqueous phase: kinetic mechanism development and modelling, *Physical Chemistry Chemical Physics*, 20, 10960–10977, <https://doi.org/10.1039/C7CP08576A>, 2018.
- Ivanova, I. P., Trofimova, S. V., Piskarev, I. M., Aristova, N. A., Burhina, O. E., and Soshnikova, O. O.: Mechanism of chemiluminescence in Fenton reaction, *Journal of Biophysical Chemistry*, 03, 88–100, <https://doi.org/10.4236/jbpc.2012.31011>, 2012.
- J. P., G.: Visual MINTEQ ver. 3.1. Preprint at (2013)., 2013.
- Kang, N., Lee, D. S., and Yoon, J.: Kinetic modeling of Fenton oxidation of phenol and monochlorophenols, *Chemosphere*, 47, 915–924, [https://doi.org/10.1016/S0045-6535\(02\)00067-X](https://doi.org/10.1016/S0045-6535(02)00067-X), 2002.
- Miller, W. L. and Kester, D. R.: Hydrogen peroxide measurement in seawater by (p-hydroxyphenyl)acetic acid dimerization, *Analytical Chemistry*, 60:24, <https://doi.org/10.1021/ac00175a014>, 1988.
- Neta, P. and Grodkowski, J.: Rate Constants for Reactions of Phenoxyl Radicals in Solution, *Journal of Physical and Chemical Reference Data*, 34, 109–199, <https://doi.org/10.1063/1.1797812>, 2005.
- Pastina, B. and LaVerne, J. A.: Effect of Molecular Hydrogen on Hydrogen Peroxide in Water Radiolysis, *The Journal of Physical Chemistry A*, 105, 9316–9322, <https://doi.org/10.1021/jp012245j>, 2001.
- Perrin, D. D.: 338. The stability of iron complexes. Part IV. Ferric complexes with aliphatic acids, *Journal of the Chemical Society (Resumed)*, 1710–1717, <https://doi.org/10.1039/JR9590001710>, 1959.
- Pontes, R. F. F., Moraes, J. E. F., Machulek, A., and Pinto, J. M.: A mechanistic kinetic model for phenol degradation by the Fenton process, *Journal of Hazardous Materials*, 176, 402–413, <https://doi.org/10.1016/j.jhazmat.2009.11.044>, 2010.
- Stookey, L. L.: Ferrozine---a new spectrophotometric reagent for iron, *Analytical Chemistry*, 42, 779–781, <https://doi.org/10.1021/ac60289a016>, 1970.
- Wang, T. L., Tong, H. W., Yan, X. Y., Sheng, L. Q., Yang, J., and Liu, S. M.: Determination of Volatile Carbonyl Compounds in Cigarette Smoke by LC-DAD, *Chromatographia*, 62, 631–636, <https://doi.org/10.1365/s10337-005-0675-8>, 2005.